



INVESTIGATION OF SINGLE PIT PROPAGATION ON 316L STAINLESS STEEL

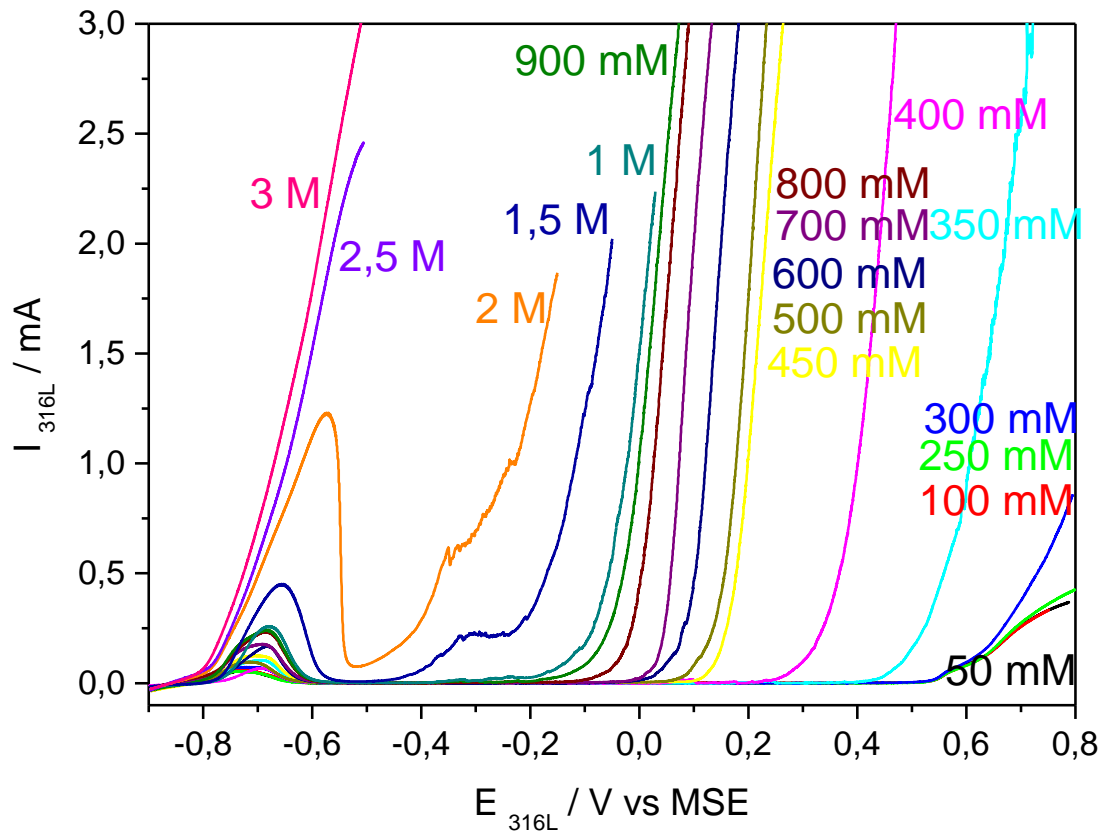
Stéphane Heurtault, Raphaël Robin, Fabien Rouillard, Vincent Vivier

LISE-CNRS-UMR 8235, Université Pierre et Marie Curie, Paris, France
CEA, DEN, DPC, SCCME, LECNA, Université Paris Saclay, Gif-sur-Yvette, France

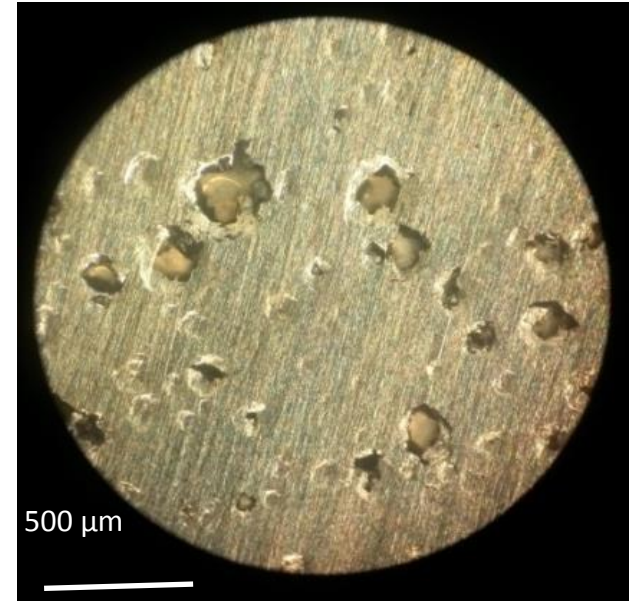
stephane.heurtault@cea.fr



Introduction



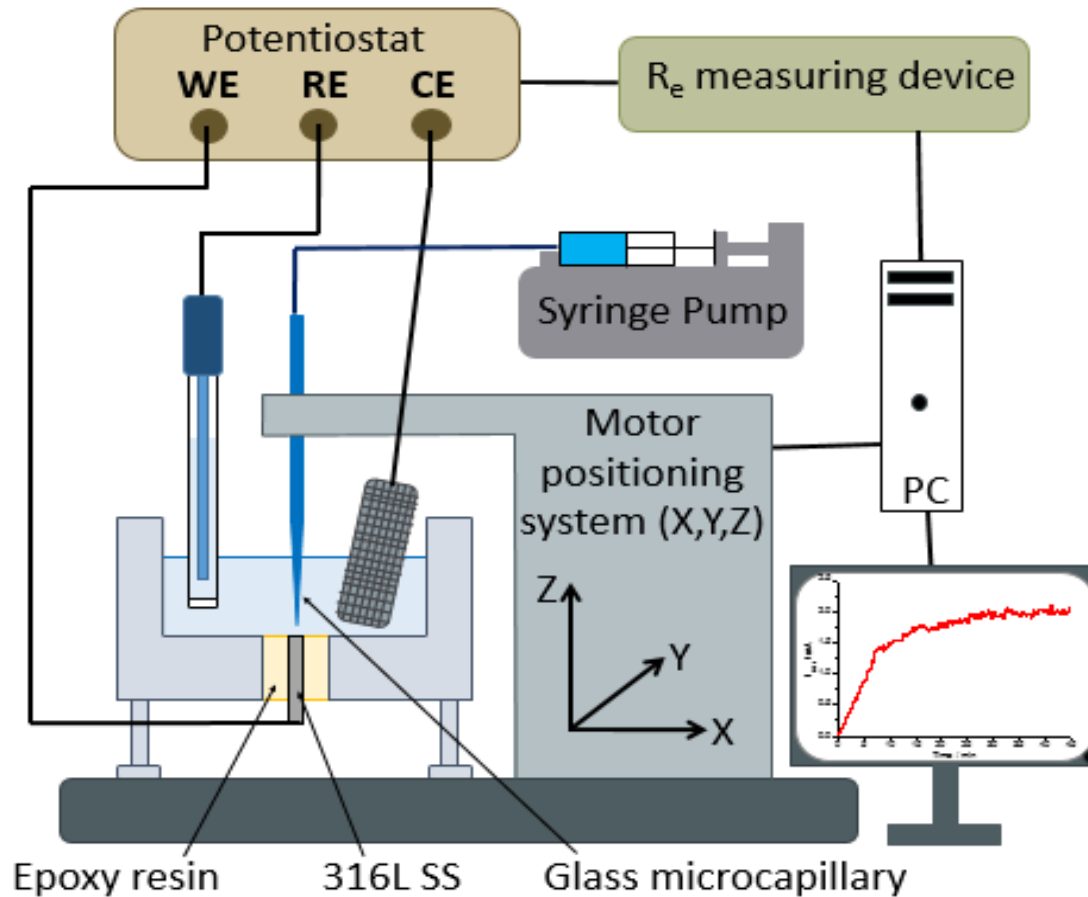
Influence of the NaCl bulk concentration on the pitting potential
Scan rate: 1 mV/s



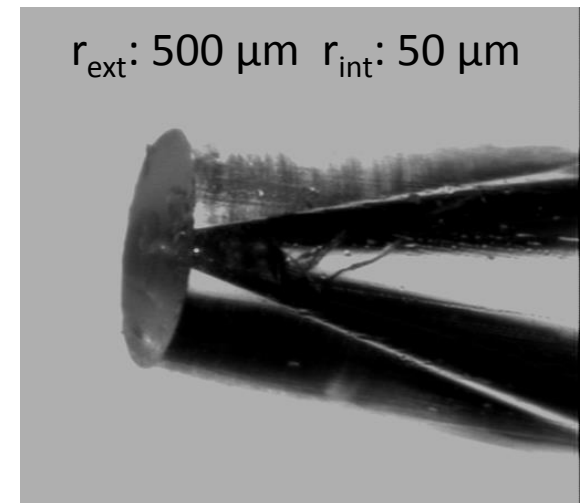
Optical image of several pits for 316L stainless steel in 0.5 M H_2SO_4 + 0.6 M NaCl

Pitting corrosion for 316L stainless steel in a chloride environment is stochastic

Experimental setup to generate a single pit



Flow microcell used to generate a single pit



Use of a glass microcapillary for controlling the amount of chloride ions in a 0.5 H_2SO_4 solution

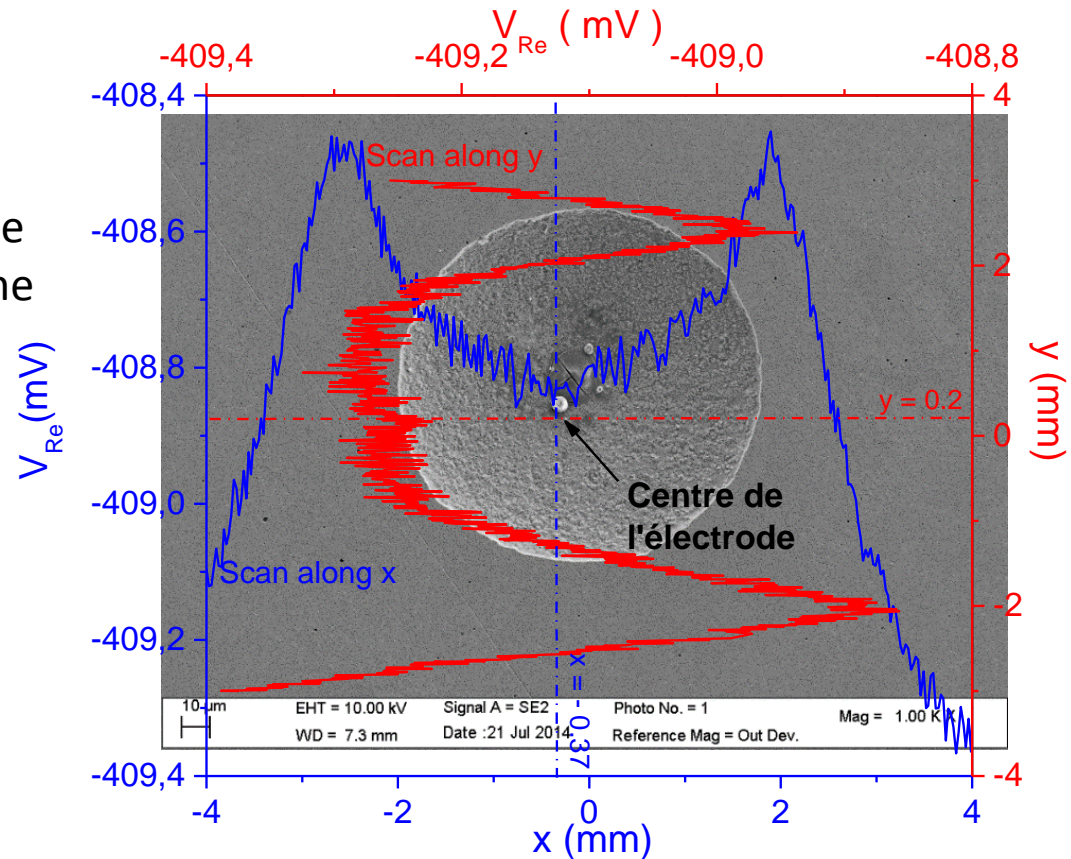
Experimental setup to generate a single pit

Microcapillary positioning

Measurement of the electrolyte resistance variation due to the presence of the capillary in the close vicinity of the stainless steel electrode

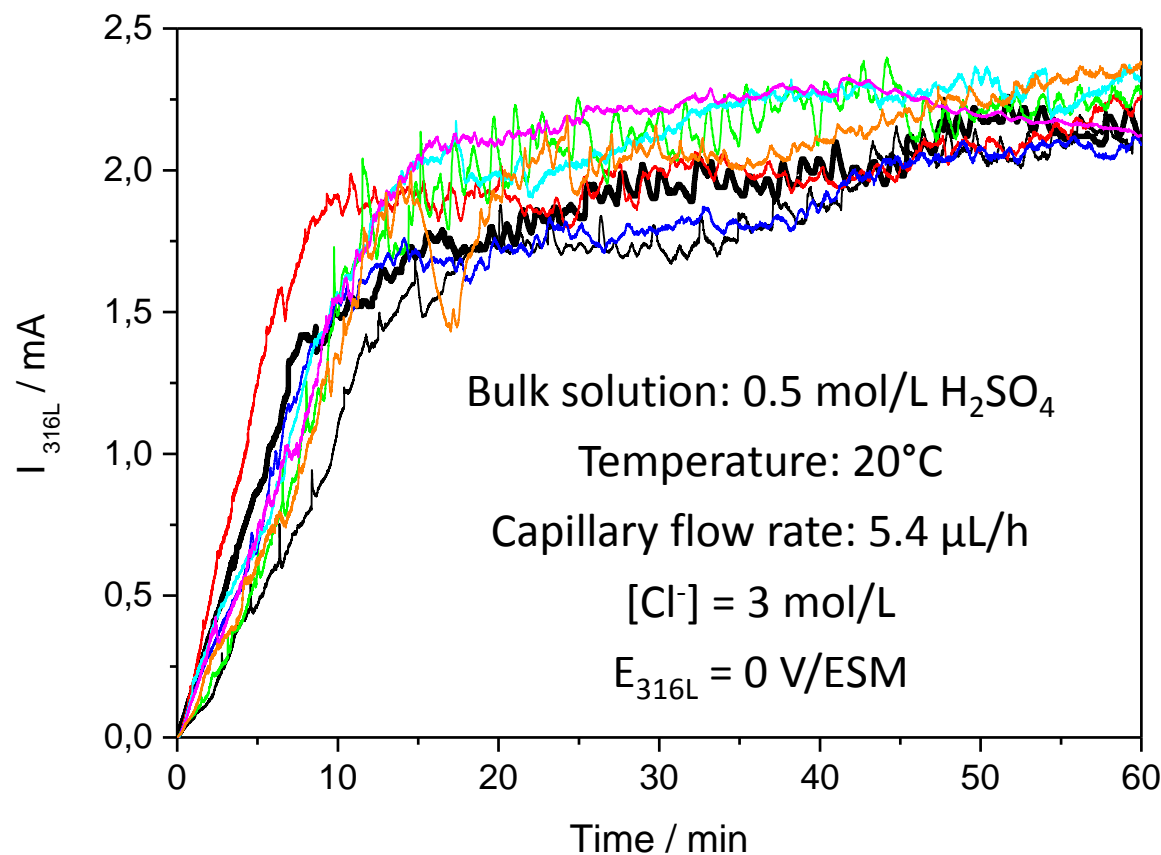
Single pit initiation

Release of chloride ions with the microcapillary in a sulfate bulk

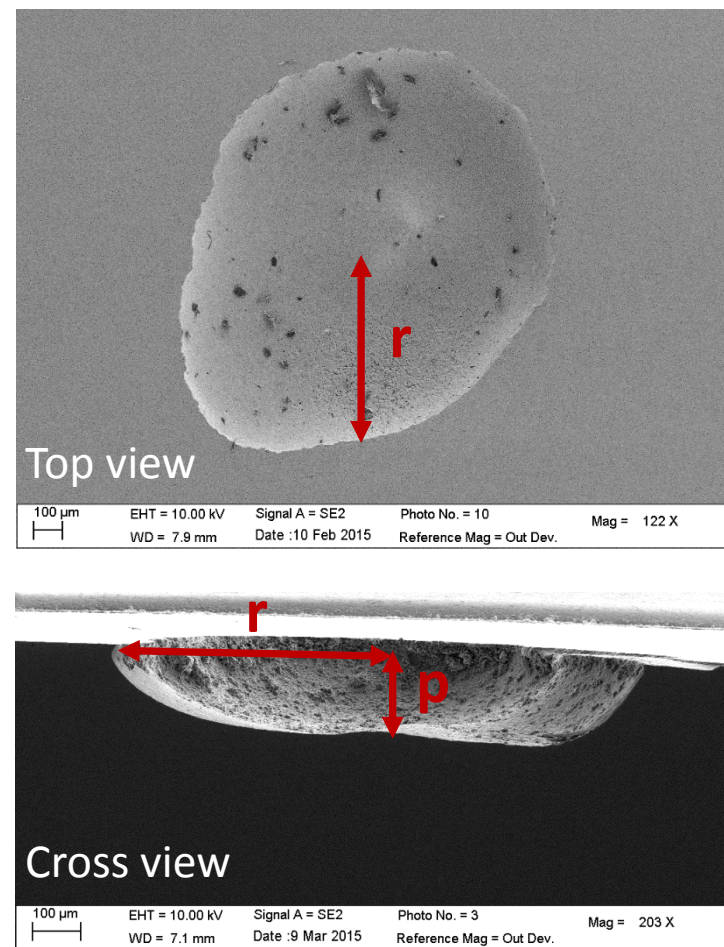


Reproducibility and characterization

Example of 7 identical experiments



Disk-shaped pit characterized by a pit radius and a pit depth



SEM observations for a single pit after 1 h of propagation

Empirical laws

From microscopy measurements

- For $t > 180$ s: pit radius

$$r(\mu\text{m}) = 250 + 26.36 * |t(s) - 180|^{0,34}$$

- For $t > 2700$ s: pit depth

$$p(\mu\text{m}) = 126 + 1.57 * |t(s) - 2700|^{0.54}$$

The depth increases with \sqrt{t}

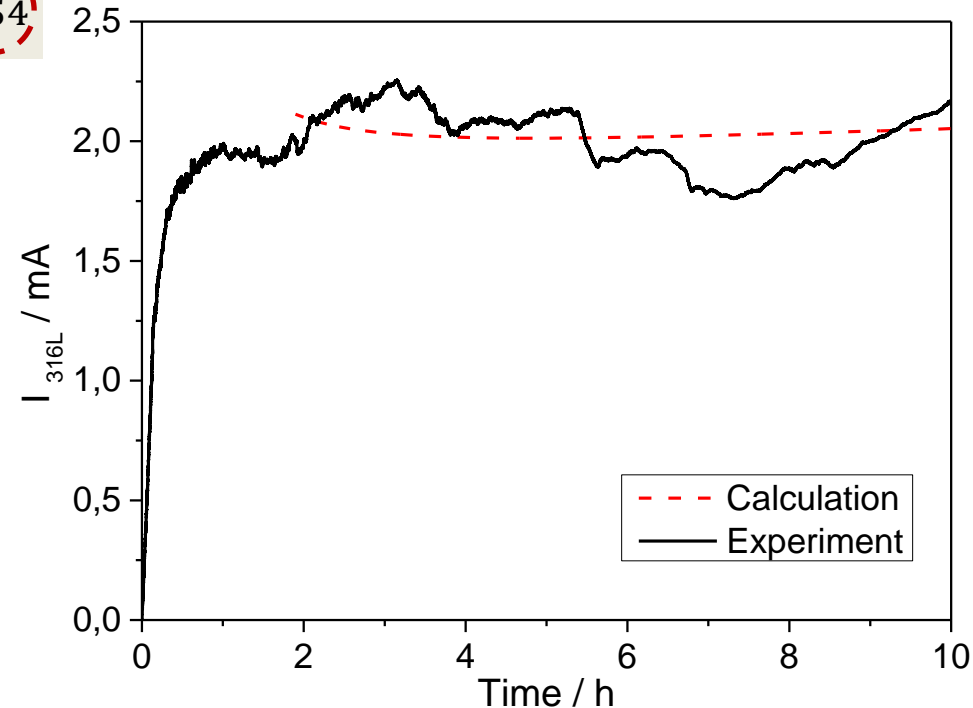
→ 2 possible limiting mechanisms:

- Diffusion
- Ohmic control

Comparison with the pitting current

$$\text{Pit volume } V_{pit} = \pi * r^2 * p$$

$$\text{Faraday's law } I = \frac{\rho n F}{M} \frac{dV}{dt}$$

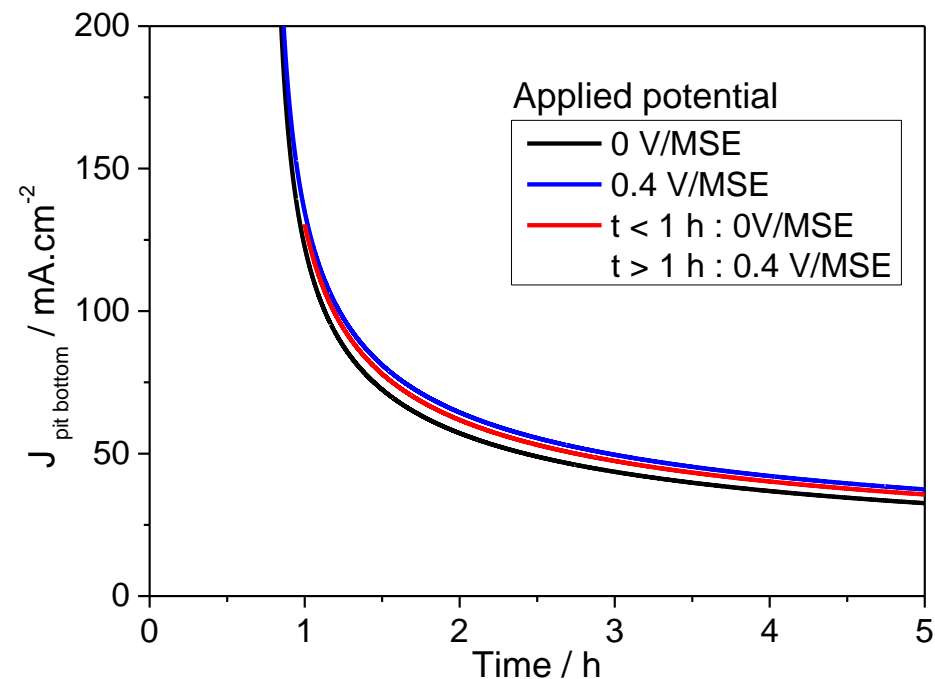


Determination of local limiting mechanisms

Parameters: 0.5 M H₂SO₄ – [Cl⁻] = 3 M – flow rate = 5.4 μL/h – 20 °C

Experiments carried out at **different applied potentials**

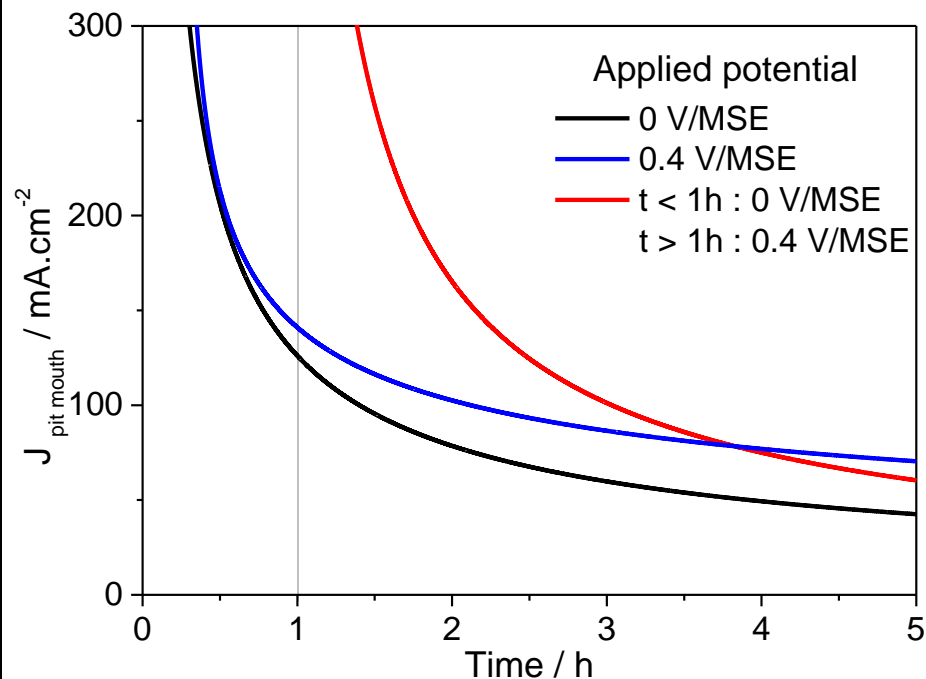
Pit bottom



Pit bottom current density not affected by the potential

→ **Diffusion controlled mechanism**

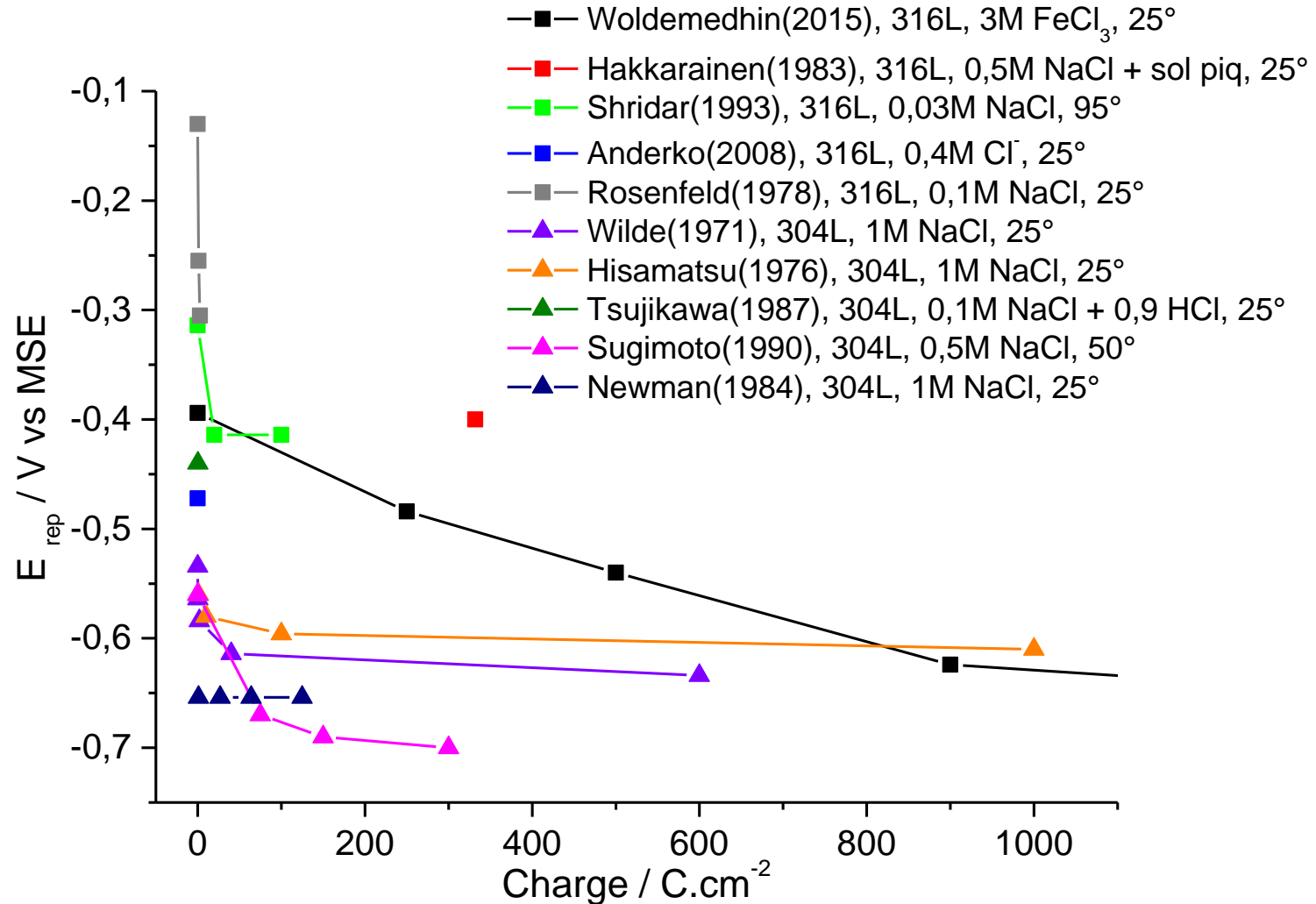
Pit mouth



Pit mouth current density affected by the potential

→ **Potential control of the pit mouth**

How to characterize the pit repassivation ?

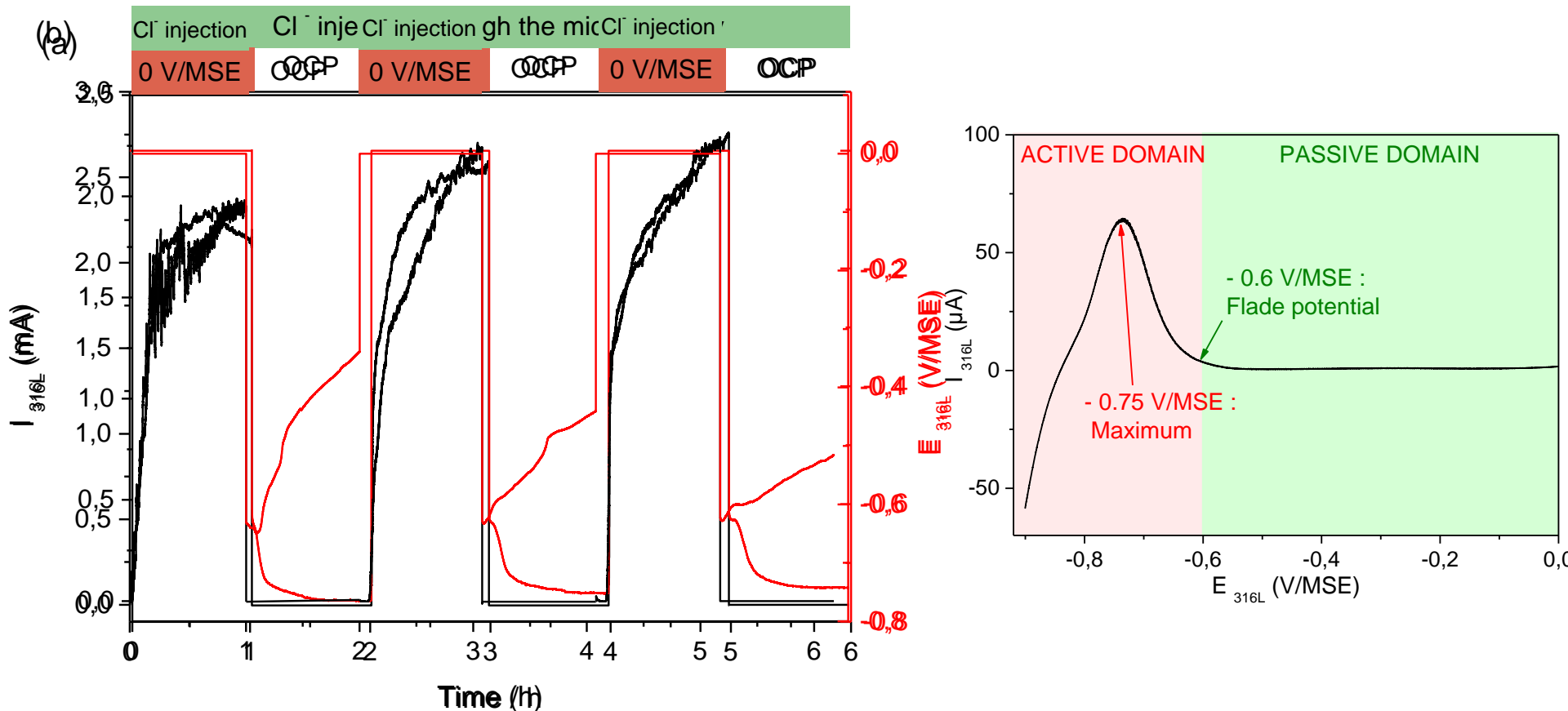


Repassivation potentials for 304L (triangle) or 316L (square) stainless steel in chloride bulk

The repassivation potential measurements can determine the pit repassivation.
Easiest repassivation for 316L than for 304L stainless steel

Role of chloride ions in pitting corrosion

Experiments performed in 0.5 M H₂SO₄ at 20°C with [Cl⁻] = 3 M (flow rate: 5.4 μL/h) and alternating OCP and polarization at 0 V/MSE



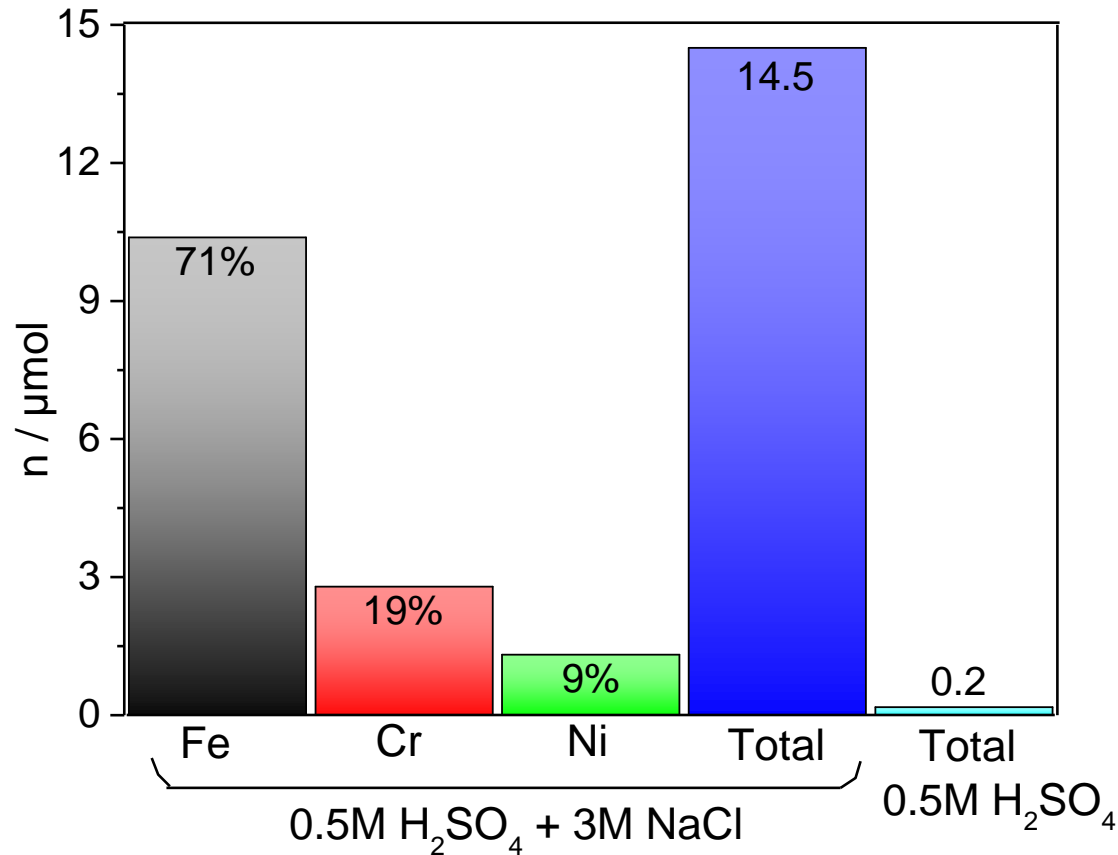
If the Cl⁻ supply is stopped, the OCP goes back to the passive domain

If the Cl⁻ supply is maintained, the OCP remains in the active domain

ICP analyses of 316L SS dissolution with and without 3M NaCl

316L SS was dissolved at OCP during 15 hours in 0.5M H₂SO₄ and 0.5M H₂SO₄ + 3M NaCl

ICP-AES analyses of bulk solutions

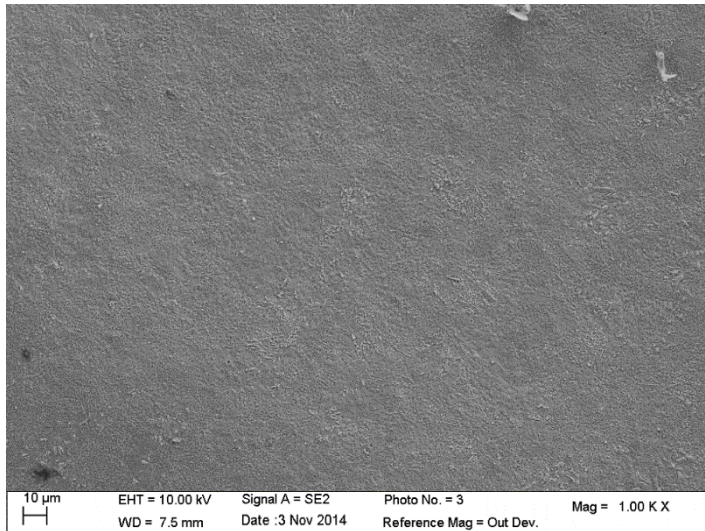


ICP analyses confirm that 3M NaCl increases the corrosion rate

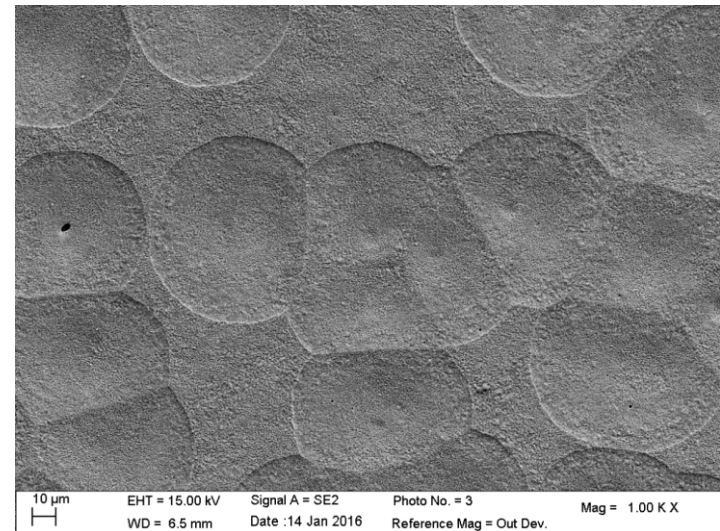
How evolves the pit during the OCP phases ?

Microscopy measurements: no evident evolution of pit depth and pit radius.

Pit bottom morphology: localized attacks in presence of Cl^-



Pit bottom after OCP without Cl^-



Pit bottom after OCP in presence of Cl^-

Slight propagation at the OCP when the Cl^- supply is maintained

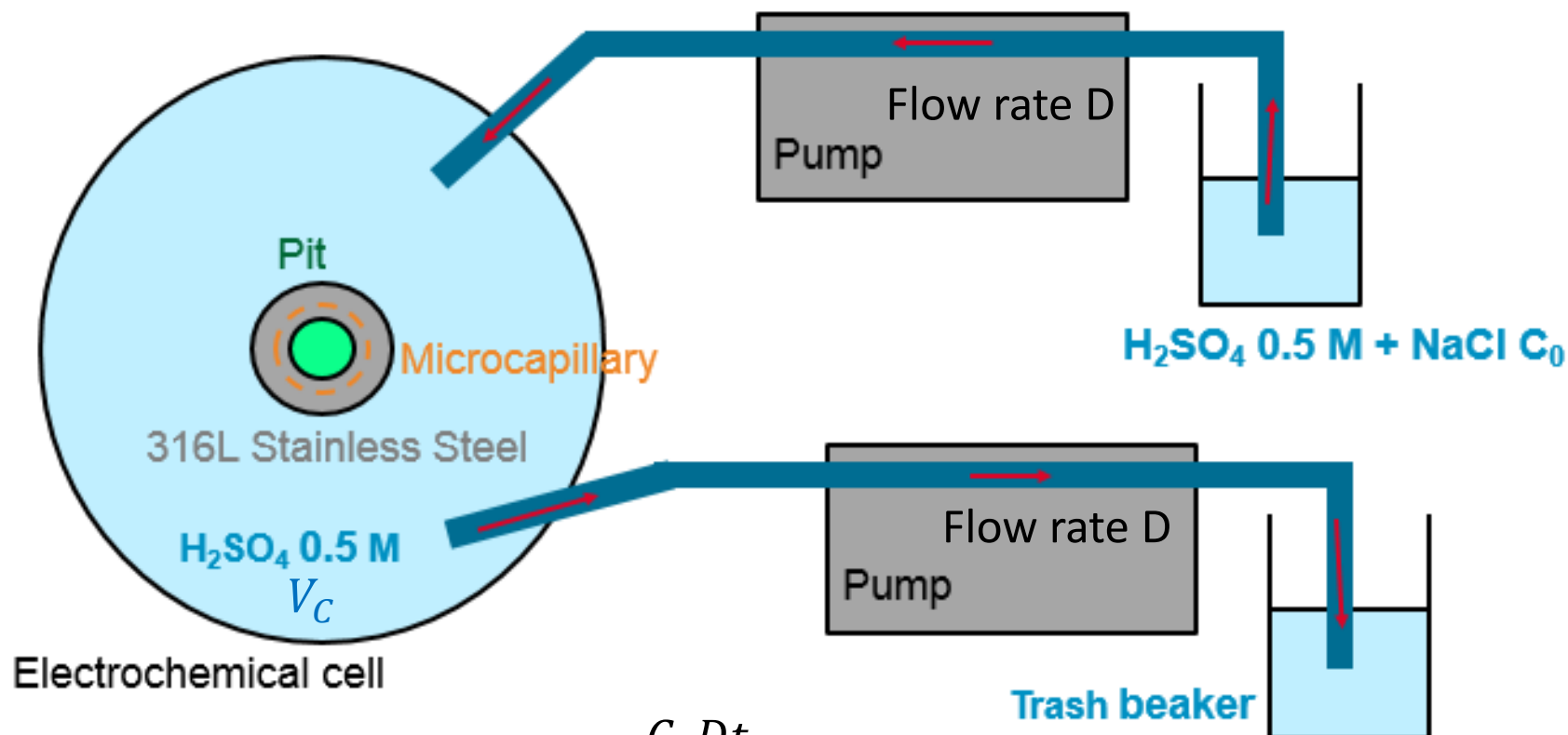
OCP recorded after a propagation + ICP analyzes + SEM images

→ **Important role of Cl^- ions in pitting corrosion**

Use of peristaltic pumps to change the solution

Experimental procedure

1. Initiation of a single pit under the microcapillary
2. Use of peristaltic pumps to change the solution from 0.5 M H_2SO_4 to 0.5 M $\text{H}_2\text{SO}_4 + C_1 \text{ NaCl}$
3. Removal of the glass microcapillary

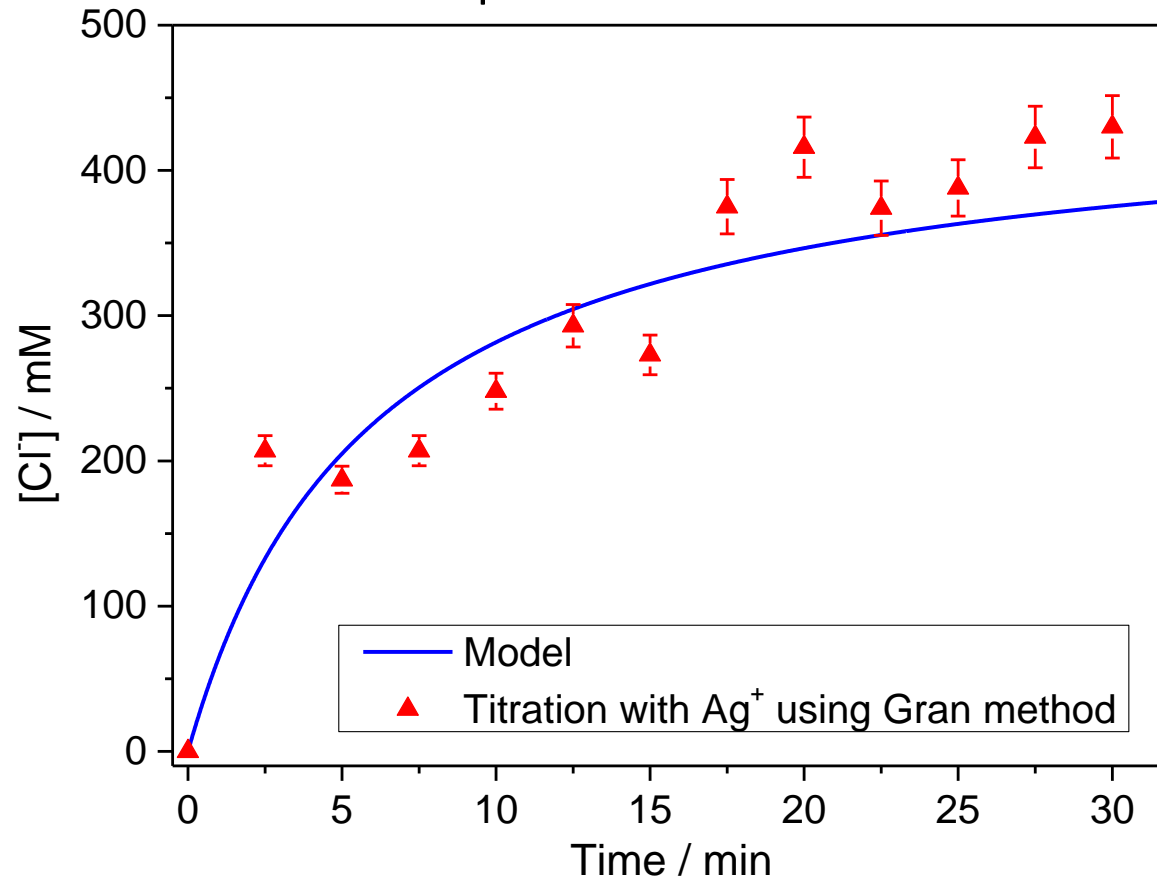


$$\text{New } [\text{Cl}^-] \text{ in the cell: } C_1 = \frac{C_0 Dt}{V_C + Dt}$$

Verification of bulk chloride concentration

$$C_0 = 450 \text{ mM NaCl} ; V_C = 40 \text{ mL} ; D = 7 \text{ mL/min}$$

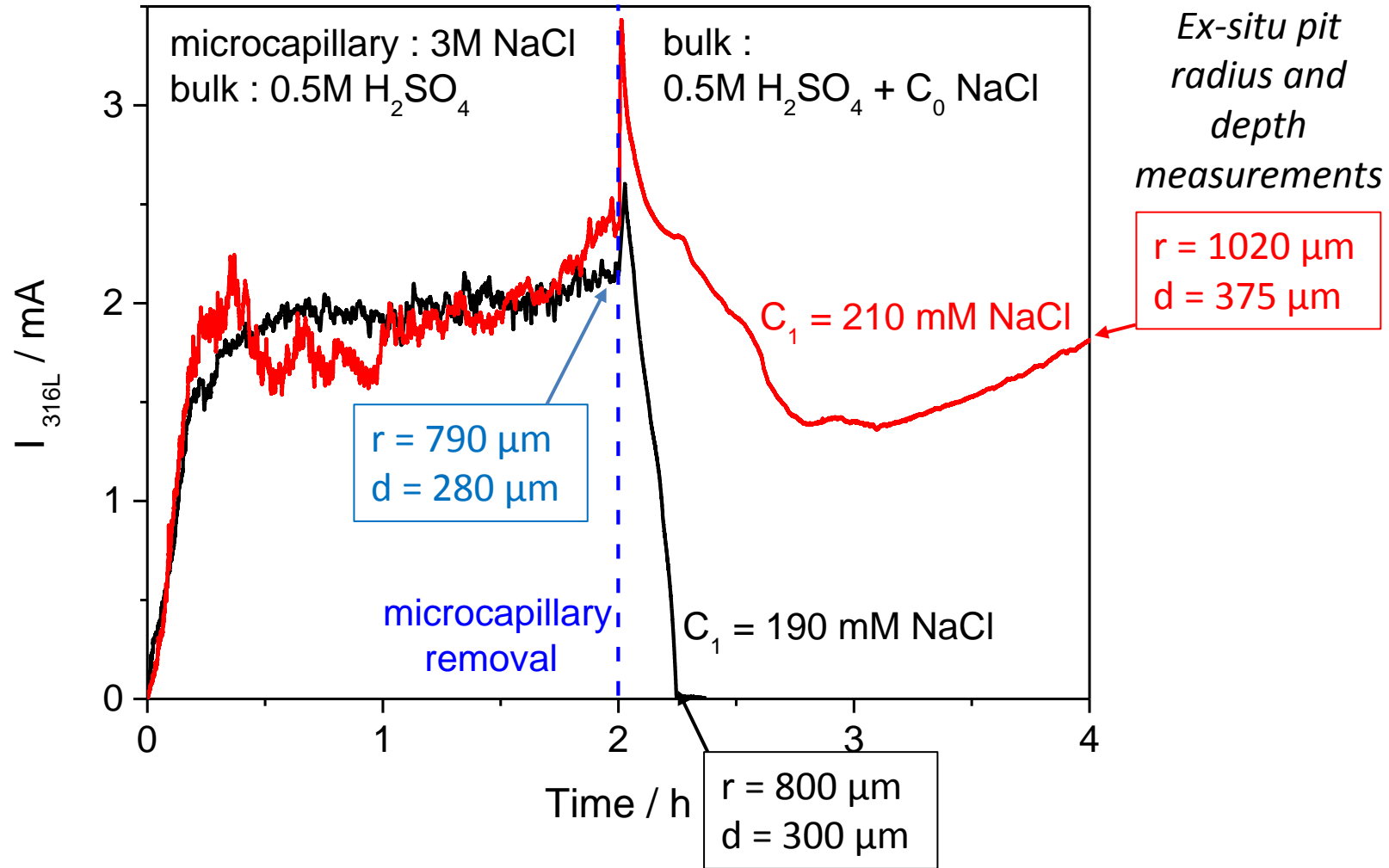
Comparison of the model with experimental results for which Cl^- titration has been performed each 2.5 min



Good prediction of the bulk chloride concentration after the use of peristaltic pumps
Measurement error: less than 5%

Determination of the repassivation Cl^- concentration

Repassivation concentration: minimum chloride concentration necessary in the bulk for sustaining the pit propagation



At 0 V/MSE and $T = 20^\circ$: **190 mM NaCl** < $C_{\text{repassivation}}$ (2 hours) < **250 mM NaCl**

Reproducible repassivation concentration

24 experiments performed
after 2 hours of propagation
 $E = 0 \text{ V/MSE}$; $T = 20^\circ$

[Cl ⁻] / mM	Propagation	Repassivation
170		1 exp
180		1 exp
190		4 exp
200	2 exp → 40 %	3 exp → 60 %
210	7 exp → 78 %	2 exp → 22 %
250	4 exp	

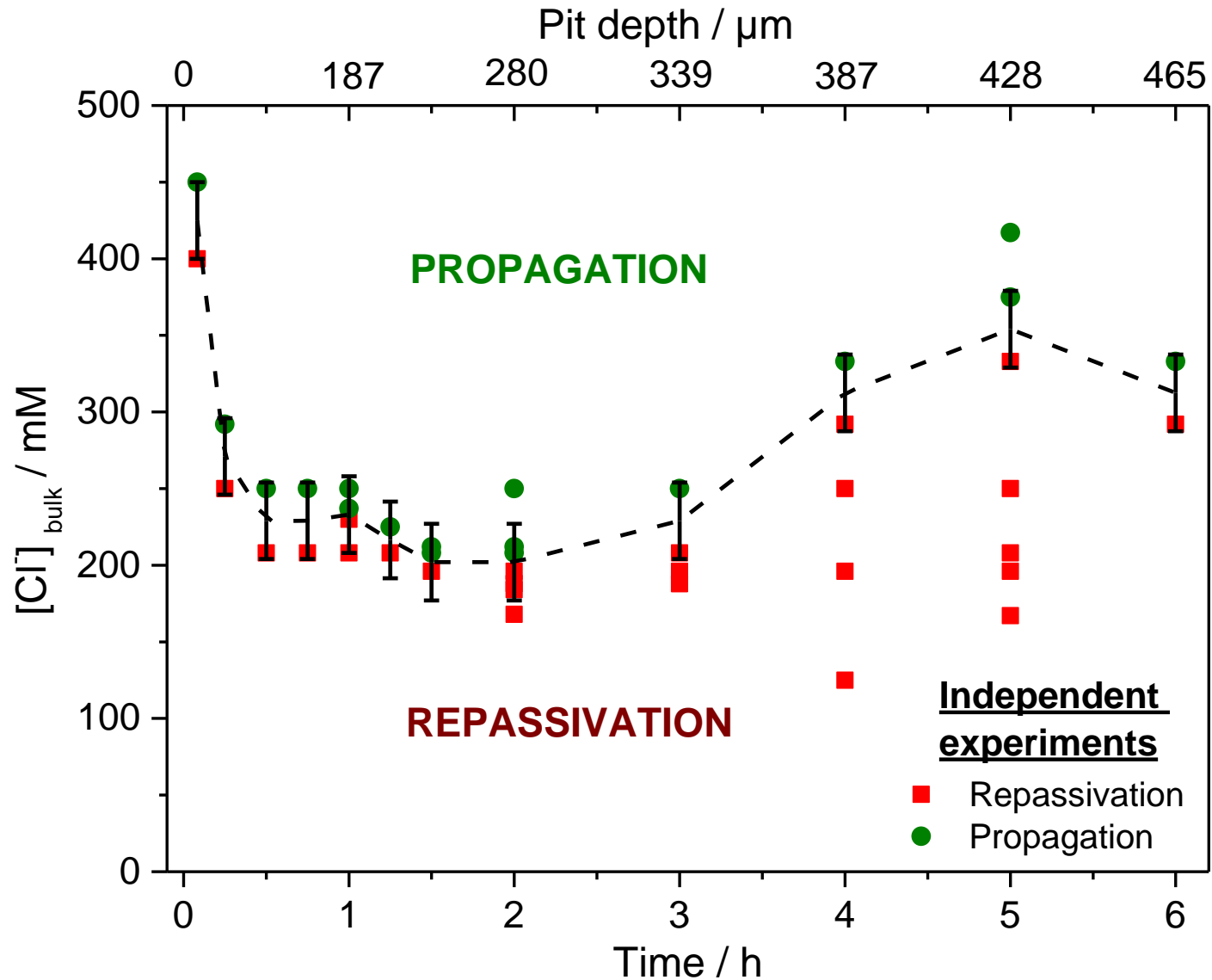
18 experiments performed
after 5 hours of propagation
 $E = 0 \text{ V/MSE}$; $T = 20^\circ$

[Cl ⁻] / mM	Propagation	Repassivation
170		1 exp
190		1 exp
210		6 exp
250		2 exp
333		3 exp
375	4 exp	
420	1 exp	

The repassivation concentration measurements are reproducible

Time evolution of the repassivation concentration

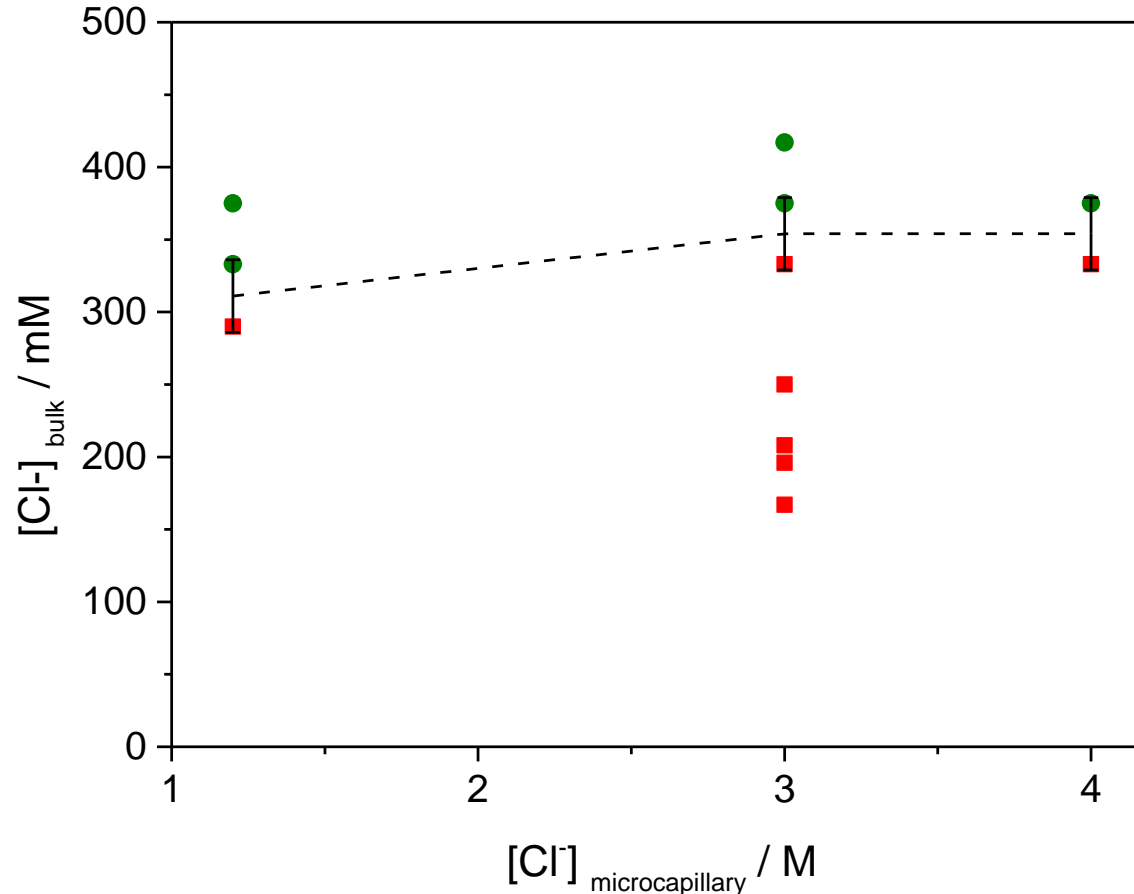
Experiments performed with $[\text{Cl}^-] = 3 \text{ M}$ at 0 V/MSE and 20°C



Influence of $[Cl^-]_{\text{microcapillary}}$ on the repassivation concentration

Experiments performed at 0 V/MSE – 20° injecting different chloride concentrations with the microcapillary for 5 hours of propagation

Flow rate: 5.4 $\mu\text{L}/\text{h}$ \rightarrow 27 μL injected during 5 hours of propagation \ll 40 mL bulk

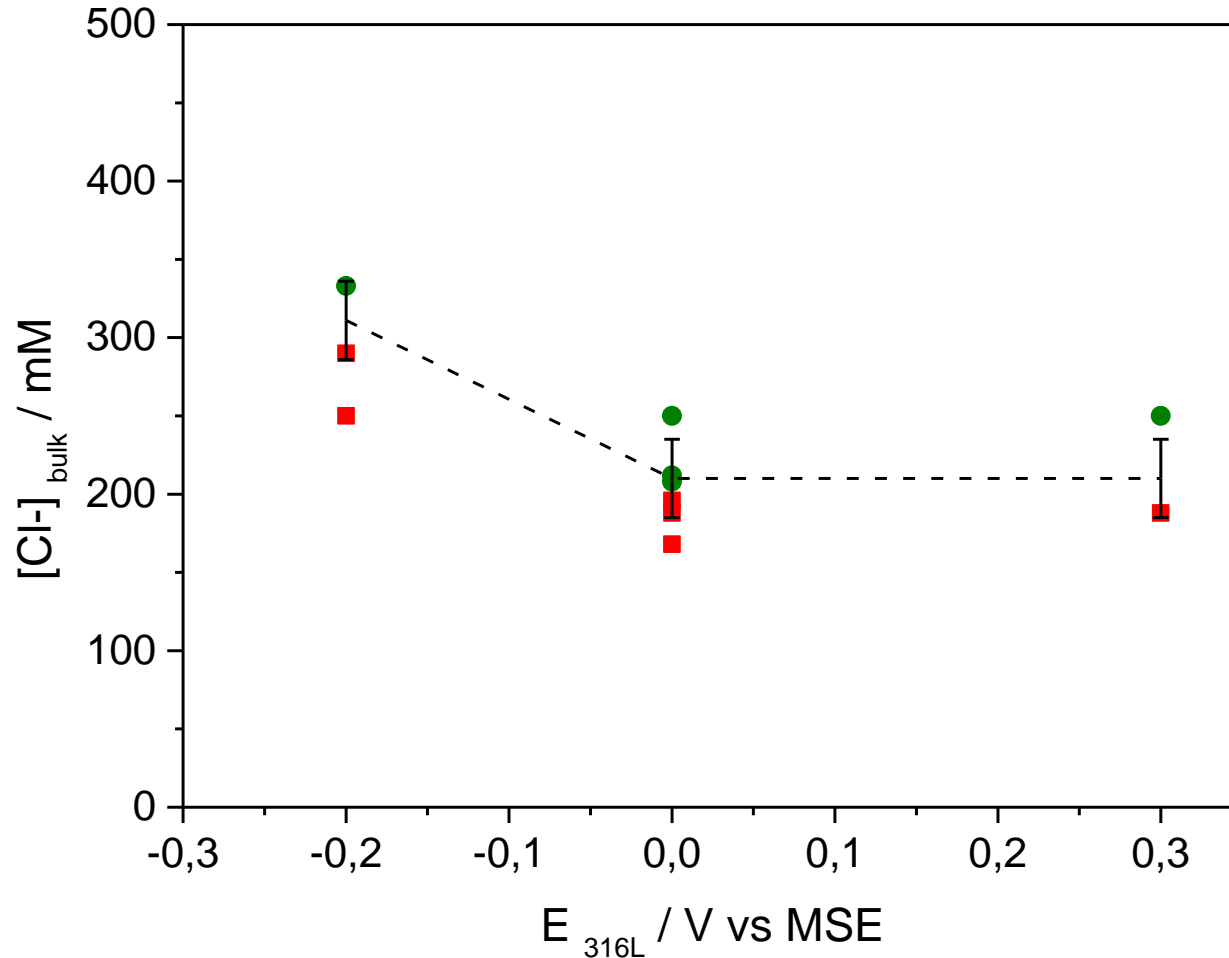


Negligible effect of $[Cl^-]$ injected by the microcapillary

Influence of potential on the repassivation concentration

20° - 2 hours of propagation - $[\text{Cl}^-]_{\text{microcapillary}}$: 3 M - Flow rate: 5.4 $\mu\text{L/h}$

Experiments for different applied potentials in the passive domain



Higher repassivation concentration in the beginning of the passive domain

Comparison with the existing work about repassivation potential

The repassivation potential is constant when a critical pit depth is reached

Literature: Determination of the dependence of E_{rep} on $[Cl^-]_{bulk}$

- *S. Tsujikawa and al., 1987 :*
304L in NaCl solution

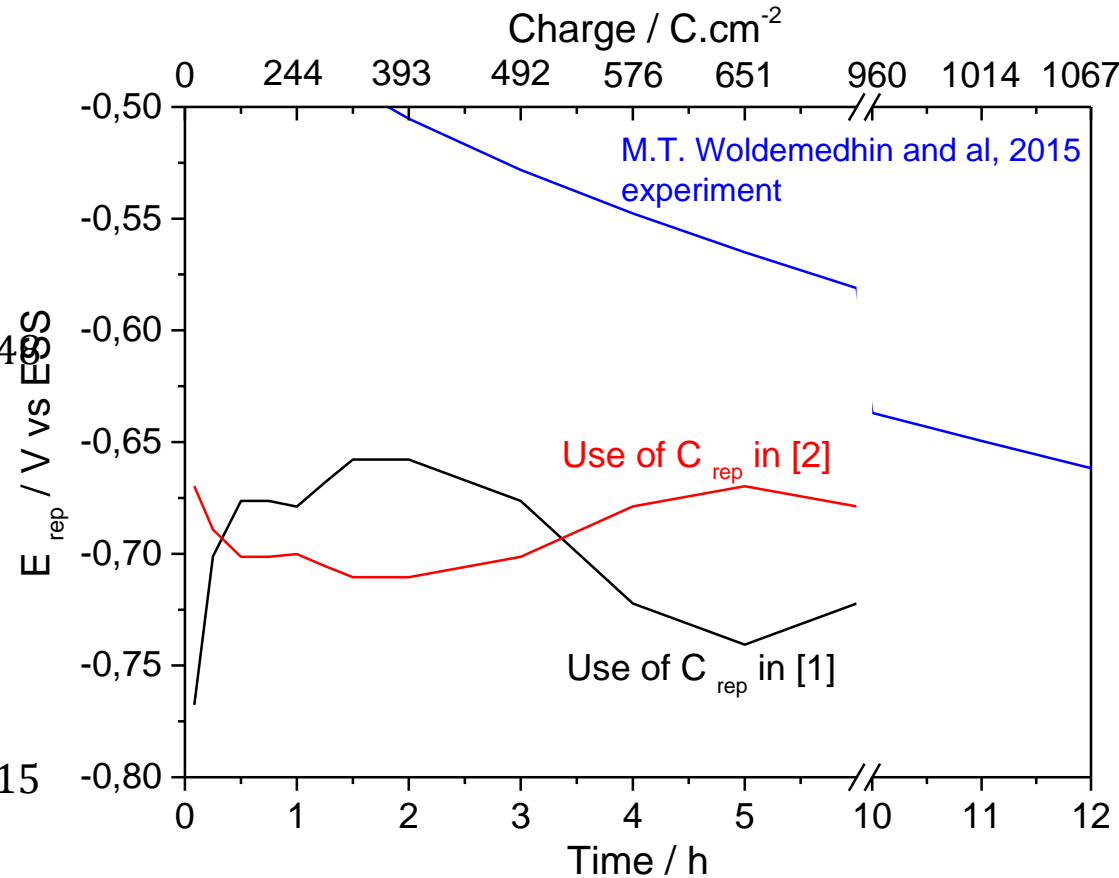
Relation [1]

$$E_{rep}(V(SCE)) = -0.34 * \log[Cl^-](mol.L^{-1}) - 0.41$$

- *M.T. Woldemedhin and al., 2015 :*
316L in $FeCl_3$

Relation [2]

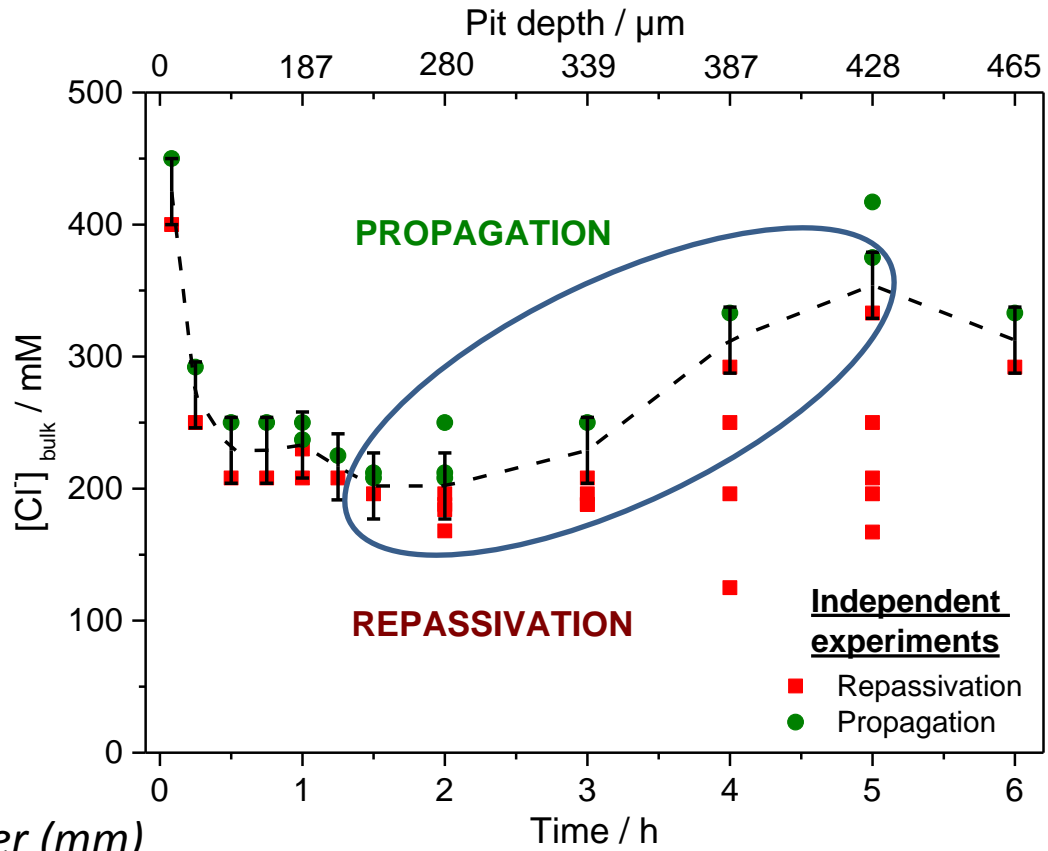
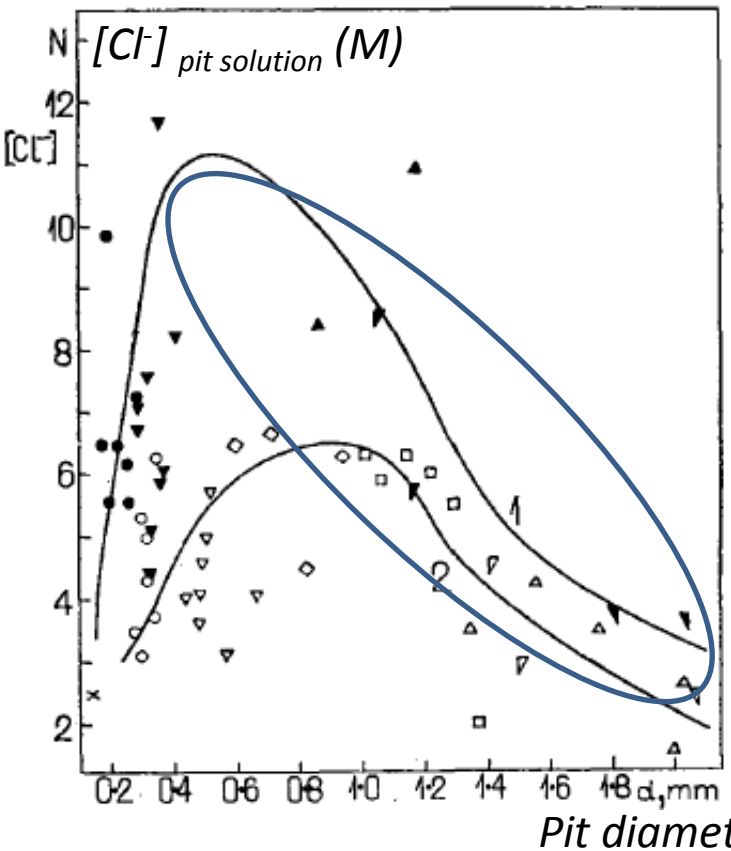
$$E_{rep}(mV(SCE)) = 55.8 * \log[FeCl_3](mol.L^{-1}) - 215$$
$$\sim 55.8 * \log[Fe^{3+}][Cl^-]^3(mol.L^{-1}) - 215$$



C_{rep} measurements consistent with a constant E_{rep}

Literature : evolution of $[Cl^-]$ in the pit solution

J. Mankowski and Z. Szklarska-Smialowska, 1975: determination of $[Cl^-]_{\text{pit solution}}$ by freezing the pit solution with solid CO_2



Decrease of $[Cl^-]$ in the pit solution while the pit is propagating
 → Link with the increase of C_{rep} above 350 μm ?

Research in progress: In-situ determination of $[Cl^-]_{\text{pit solution}}$ with microelectrodes

Conclusions

- Initiation and propagation of a reproducible single pit on 316L stainless steel using a flow microcell setup
- Determination of single pit propagation mechanisms:
 - Pit bottom: diffusion
 - Pit mouth: potential control
- Important role of chloride ion in pitting corrosion processes
- Characterization of pit repassivation by bulk chloride concentration
 - Definition of a repassivation concentration C_{rep}
 - Reproducible measurement
 - Evolution of C_{rep} with pit depth (for $20^\circ - 0$ V/MSE) :
 - Below $120 \mu\text{m}$: decrease of C_{rep}
 - Between $120 \mu\text{m}$ and $350 \mu\text{m}$: constant C_{rep}
 - Above $350 \mu\text{m}$: increase of C_{rep}
 - No influence of $[\text{Cl}^-]_{microcapillary}$ on C_{rep}
 - Higher C_{rep} at the beginning of the passive range

